

# Comparative genomics reveals the *in planta*-secreted *Verticillium dahliae* Av2 effector protein recognized in tomato plants that carry the V2 resistance locus

Edgar A. Chavarro-Carrero,<sup>1†</sup> Jasper P. Vermeulen,<sup>1,2†</sup>

David E. Torres,<sup>1,3</sup> Toshiyuki Usami,<sup>4</sup>

Henk J. Schouten,<sup>2</sup> Yuling Bai,<sup>2</sup> Michael F. Seidl<sup>1,3†</sup>

and Bart P. H. J. Thomma  <sup>1,5\*</sup>†

<sup>1</sup>Laboratory of Phytopathology, Wageningen University and Research, Wageningen, 6708 PB, The Netherlands.

<sup>2</sup>Laboratory of Plant Breeding, Wageningen University and Research, Wageningen, 6708 PB, The Netherlands.

<sup>3</sup>Theoretical Biology and Bioinformatics Group, Department of Biology, Utrecht University, Utrecht, The Netherlands.

<sup>4</sup>Graduate School of Horticulture, Chiba University, Matsudo, Chiba, 271-8510, Japan.

<sup>5</sup>Cluster of Excellence on Plant Sciences (CEPLAS), University of Cologne, Botanical Institute, Cologne, Germany.

## Summary

Plant pathogens secrete effector molecules during host invasion to promote colonization. However, some of these effectors become recognized by host receptors to mount a defence response and establish immunity. Recently, a novel resistance was identified in wild tomato, mediated by the single dominant V2 locus, to control strains of the soil-borne vascular wilt fungus *Verticillium dahliae* that belong to race 2. With comparative genomics of race 2 strains and resistance-breaking race 3 strains, we identified the avirulence effector that activates V2 resistance, termed Av2. We identified 277 kb of race 2-specific sequence comprising only two genes encoding predicted secreted proteins that are expressed during tomato colonization. Subsequent functional analysis based on genetic complementation into race 3 isolates and targeted deletion from the race 1 isolate JR2 and race 2 isolate TO22 confirmed that one of the two candidates encodes the avirulence effector Av2 that is recognized in V2

tomato plants. Two Av2 allelic variants were identified that encode Av2 variants that differ by a single acid. Thus far, a role in virulence could not be demonstrated for either of the two variants.

## Introduction

In nature, plants are continuously threatened by potential plant pathogens. However, most plants are resistant to most potential plant pathogens due to an efficient immune system that becomes activated by any type of molecular pattern that accurately betrays microbial invasion (Dangl and Jones, 2001; Cook et al., 2015). Throughout time, different conceptual frameworks have been put forward to describe the molecular basis of plant–pathogen interactions and the mechanistic underpinning of plant immunity. Initially, Harold Flor introduced the gene-for-gene model in which a single dominant host gene, termed a resistance (*R*) gene, induces resistance in response to a pathogen expressing a single dominant avirulence (*Avr*) gene (Flor, 1942). Isolates of the pathogen that do not express the allele of the *Avr* gene that is recognized escape recognition and are assigned to a resistance-breaking race. In parallel to these race-specific *Avrs*, non-race-specific elicitors were described as conserved microbial molecules that are often recognized by multiple plant species (Darvill and Albersheim, 1984). The recognition by plants of *Avrs* and of non-race-specific elicitors, presently known as pathogen- or microbe-associated molecular patterns (P/MAMPs), was combined in the ‘zig-zag’ model (Jones and Dangl, 2006). In this model, P/MAMPs are perceived by cell surface-localized pattern recognition receptors (PRRs) to trigger pattern-triggered immunity (PTI), while effectors are recognized by cytoplasmic receptors that are known as resistance (*R*) proteins to activate effector-triggered immunity (ETI) (Jones and Dangl, 2006). Importantly, the model recognizes that *Avrs* function to suppress host immune responses in the first place, implying that these molecules, besides being avirulence determinants, act as virulence factors through their function as effector molecules (Jones and Dangl, 2006). A more recent model, termed the invasion model, recognizes that the functional separation of

Received 11 September, 2020; revised 16 October, 2020; accepted 18 October, 2020. \*For correspondence. E-mail bart.thomma@wur.nl; Tel. (+0031) 317 484536; Fax (+0031) 317 483412. <sup>†</sup>These authors contributed equally to this work.

PTI and ETI is problematic and proposes that the corresponding receptors, collectively termed invasion pattern receptors (IPRs), detect either externally encoded or self-modified ligands that indicate invasion, termed invasion patterns (IPs), to mount an effective immune response (Thomma et al., 2011; Cook et al., 2015). However, it is generally appreciated that microbial pathogens secrete dozens to hundreds of effectors to contribute to disease establishment, only some of which are recognized as Avrs (Rovenich et al., 2014).

IPRs encompass typical *R* genes, which have been exploited for almost a century to confer resistance against plant pathogens upon introgression from sexually compatible wild relatives into elite cultivars (Dodds and Rathjen, 2010; Dangl et al., 2013). Most *R* genes encode members of a highly polymorphic superfamily of intracellular nucleotide-binding leucine-rich repeat (NLR) receptors, while others encode cell surface receptors (Dangl et al., 2013). Unfortunately, most *R* genes used in commercial crops are short-lived because the resistance that they provide is rapidly broken by pathogen populations as their deployment in monoculture-based cropping systems selects for pathogen variants that overcome immunity (Stukenbrock and McDonald, 2008; Dangl et al., 2013). Such breaking of resistance occurs upon purging of the *Avr* gene, sequence diversification, or by employment of novel effectors that subvert the host immune response (Stergiopoulos et al., 2007; Cook et al., 2015).

The molecular cloning of the first bacterial *Avr* gene from *Pseudomonas syringae* pv. *glycinea* was reported in 1984 (Staskawicz et al., 1984), the first fungal *Avr* gene from *Cladosporium fulvum* in 1991 (van Kan et al., 1991) and the first oomycete *Avr* gene from *Phytophthora sojae* in 2004 (Shan et al., 2004). Dozens of additional *Avr* genes have been cloned since then, in various pathogens (Parlange et al., 2009; Inami et al., 2012; Plissonneau et al., 2016; Niu et al., 2016; Lu et al., 2016; Zhong et al., 2017; Salcedo et al., 2017; Praz et al., 2016; Inoue et al., 2017; Chen et al., 2017; Meile et al., 2018; Kema et al., 2018; Anh et al., 2018; Bourras et al., 2015, 2019; Petit-Houdenot et al., 2019; Saur et al., 2019). Most of these *Avr* genes have been identified by map-based cloning and reverse genetics strategies. More recently, advances in (the affordability of) genome sequencing have allowed the cloning of novel Avrs by combining comparative genomics or transcriptomics with functional assays, a trend that was spearheaded by the cloning of the first *Avr* gene from *Verticillium dahliae* only in 2012 (de Jonge et al., 2012; Mesarich et al., 2014; Schmidt et al., 2016).

*Verticillium dahliae* is a soil-borne fungal pathogen and causal agent of *Verticillium* wilt on a broad range of host plants that comprises hundreds of dicotyledonous plant species, including numerous crops such as tomato, potato,

lettuce, olive, and cotton (Fradin and Thomma, 2006; Klosterman et al., 2009). The first source of genetic resistance toward *Verticillium* wilt was identified in tomato (*Solanum lycopersicum*) in the early 1930s in an accession called Peru Wild (Schaible et al., 1951). The resistance is governed by a single dominant locus, designated *Ve* (Diwan et al., 1999), comprising two genes that encode cell surface receptors of which one, *Ve1*, acts as a genuine resistance gene (Fradin and Thomma, 2006). Shortly after its deployment in the 1950s, resistance-breaking strains have appeared that were assigned to race 2, whereas strains that are contained by *Ve1* belong to race 1 (Alexander, 1962). Thus, *Ve1* is characterized as a race-specific *R* gene, and resistance-breaking strains have become increasingly problematic over time (Alexander, 1962; Dobinson et al., 1996). With comparative population genomics of race 1 and race 2 strains, the *V. dahliae* avirulence effector that is recognized by tomato *Ve1* was identified as *VdAve1*, an effector that is secreted during host colonization (de Jonge et al., 2012). As anticipated, it was demonstrated that *VdAve1* acts as a virulence factor on tomato plants that lack the *Ve1* gene and that, consequently, cannot recognize *VdAve1* (de Jonge et al., 2012). Recent evidence demonstrates that *VdAve1* exerts selective antimicrobial activity and has the capacity to manipulate local microbiomes inside host plants as well as in the environment (Snelders et al., 2020). Whereas all race 1 strains carry an identical copy of *VdAve1*, all race 2 strains analysed to date are characterized by complete loss of the *VdAve1* locus (de Jonge et al., 2012; Faino et al., 2016). Intriguingly, phylogenetic analysis has revealed that *VdAve1* was horizontally acquired by *V. dahliae* from plants (de Jonge et al., 2012; Shi-Kunne et al., 2018), after which the effector gene was lost multiple times independently, presumably due to selection pressure exerted by the *Ve1* locus that has been introgressed into most tomato cultivars (Faino et al., 2016).

Despite significant efforts, attempts to identify genetic sources for race 2 resistance in tomato have remained unsuccessful for a long time (Baergen et al., 1993). Recently, however, a source of race 2 resistance was identified in the wild tomato species *Solanum neorickii* (Usami et al., 2017). This genetic material was used to develop the tomato rootstock cultivars Aibou, Ganbarune-Karis and Back Attack by Japanese breeding companies, in which resistance is controlled by a single dominant locus, denoted *V2* (Usami et al., 2017). However, experimental trials using race 2-resistant rootstocks revealed resistance-breaking *V. dahliae* strains that, consequently, are assigned to race 3 (Usami et al., 2017). In this study, we performed comparative genomics combined with functional assays to identify the avirulence effector *Av2* that activates race-specific resistance in tomato genotypes that carry *V2*.

## Results

### *Identification of *Verticillium dahliae* strains that escape V2 resistance*

To identify *Av2* as the *V. dahliae* gene that mediates avirulence on tomato *V2* plants, we pursued a comparative genomics strategy by searching for genomic regions that are absent from all race 3 strains. To this end, we performed pathogenicity assays with a collection of *V. dahliae* strains on a differential set of tomato genotypes, comprising (I) Moneymaker plants that lack *V. dahliae* resistance genes, (II) *Ve1*-transgenic Moneymaker plants that are resistant against race 1 and not against race 2 strains (Fradin *et al.*, 2009), and (III) Aibou plants that carry *Ve1* and *V2* and are therefore resistant against race 1 as well as race 2 strains (Usami *et al.*, 2017) (Fig. 1A). First, we aimed to confirm the race assignment of eight *V. dahliae* strains that were previously tested by Usami *et al.* (2017) (Table 1). Additionally, three strains that were previously assigned to race 2 were included (de Jonge *et al.*, 2012) as well as *V. dahliae* strain JR2 (race 1) because of its gapless telomere-to-telomere assembly (Faino *et al.*, 2015).

At 3 weeks post inoculation, all strains caused significant stunting on the universally susceptible Moneymaker control (Fig. 1A and B), while all strains except for the race 1 strain JR2 caused significant stunting on *Ve1*-transgenic Moneymaker plants (Fig. 1A and C), corroborating that, except for strain JR2, none of the strains belongs to race 1 and that a potential containment on Aibou plants cannot be caused by *Ve1* recognition of the *VdAve1* effector. Importantly, all of the strains that were used by Usami *et al.* (2017) and that were previously assigned to race 2 did not cause significant stunting on Aibou, whereas all of the strains that were assigned to race 3 caused clear symptoms of *Verticillium* wilt disease (Fig. 1, Table 1; Usami *et al.*, 2017). The previously assigned race 2 strain DVDS26 (de Jonge *et al.*, 2012) caused no significant stunting on Aibou plants, confirming that this remains a race 2 strain, while strains DVD161 and DVD3 caused significant stunting, implying that these strains should actually be assigned to race 3. As expected, the race 1 strain JR2 did not cause stunting on Aibou plants, which can at least partially be attributed to *VdAve1* effector recognition by the *Ve1* gene product in these plants. However, the finding that a transgenic *VdAve1* deletion line (JR2 $\Delta$ Ave1; de Jonge *et al.*, 2012) caused significant stunting on *Ve1*-transgenic Moneymaker and not on Aibou plants, indicates that the JR2 strain might also encode *Av2*. Currently, it is not known whether this is the case, or whether it is simply that basal defence is enhanced in the absence of *Ave1*. After all, we previously showed that the virulence of the *VdAve1* deletion strain on tomato is severely compromised (de Jonge

*et al.*, 2012), which can also be observed on Moneymaker plants in our assays (Fig. 1B). This observation, combined with the observation that stunting on Aibou plants by any race 3 strain is generally less than stunting on Moneymaker plants (Fig. 1B and D), could indicate that basal defence against *Verticillium* wilt is enhanced in Aibou plants, and thus that incompatibility of the *VdAve1* deletion strain may be due to enhanced basal defence rather than due to *V2*-mediated recognition of the JR2 strain.

### *Comparative genomics identifies *Verticillium dahliae* Av2 candidates*

Besides the gapless genome assembly of strain JR2 (Faino *et al.*, 2015), genome assemblies were also available for strains DVDS26, DVD161 and DVD3, albeit that these assemblies were highly fragmented as these were based on Illumina short-read sequencing data (de Jonge *et al.*, 2012) (Table 1). In this study, we determined the genomic sequences of the race 2 strains TO22, UD1-4-1, GF1207 and GFCA2, and the race 3 strains GF-CB5, GF1192, VT2A and HOMCF with Oxford Nanopore sequencing Technology (ONT) using a MinION device (Table 1). For each strain, ~2–4 Gb of sequence data was produced, representing 50–100x genome coverage based on the ~35 Mb gapless reference genome of *V. dahliae* strain JR2 (Faino *et al.*, 2015). Subsequently, we performed self-correction of the reads, read trimming and genome assembly, leading to genome assemblies ranging from 18 contigs for strain UD1-4-1 to 69 for strain GF1207 (Table 1).

Based on the genome sequences, we pursued comparative genomics analyses by exploring two scenarios. The first scenario is that *Av2* is race 2-specific and thus present in race 2 lineage sequences while absent from race 3. The second scenario is that *Av2* is present in isolates that belong to race 1 and race 2, but that the resistance phenotype against race 2 is masked by *Ve1* resistance directed against *Ave1*. In scenario I, comparative genomics was performed making use of race 2 strain TO22 (Usami *et al.*, 2017) as a reference, while in scenario II race 1 strain JR2 (Faino *et al.*, 2015) was used (Table 2). To this end, self-corrected reads from the *V. dahliae* race 3 strains were mapped against the assembly of *V. dahliae* strain TO22 (scenario I) or strain JR2 (scenario II) and regions that were not covered by race 3 reads were retained (Table 2). Next, self-corrected reads from the race 2 strains were mapped against the retained reference genome-specific regions that are absent from the race 3 strains, and sequences that were found in every race 2 strain were retained as candidate regions to encode the *Avr* molecule. Sequences that are shared by the *V. dahliae* strain TO22 reference assembly and all race 2 strains, and that are absent from all race 3 strains, were

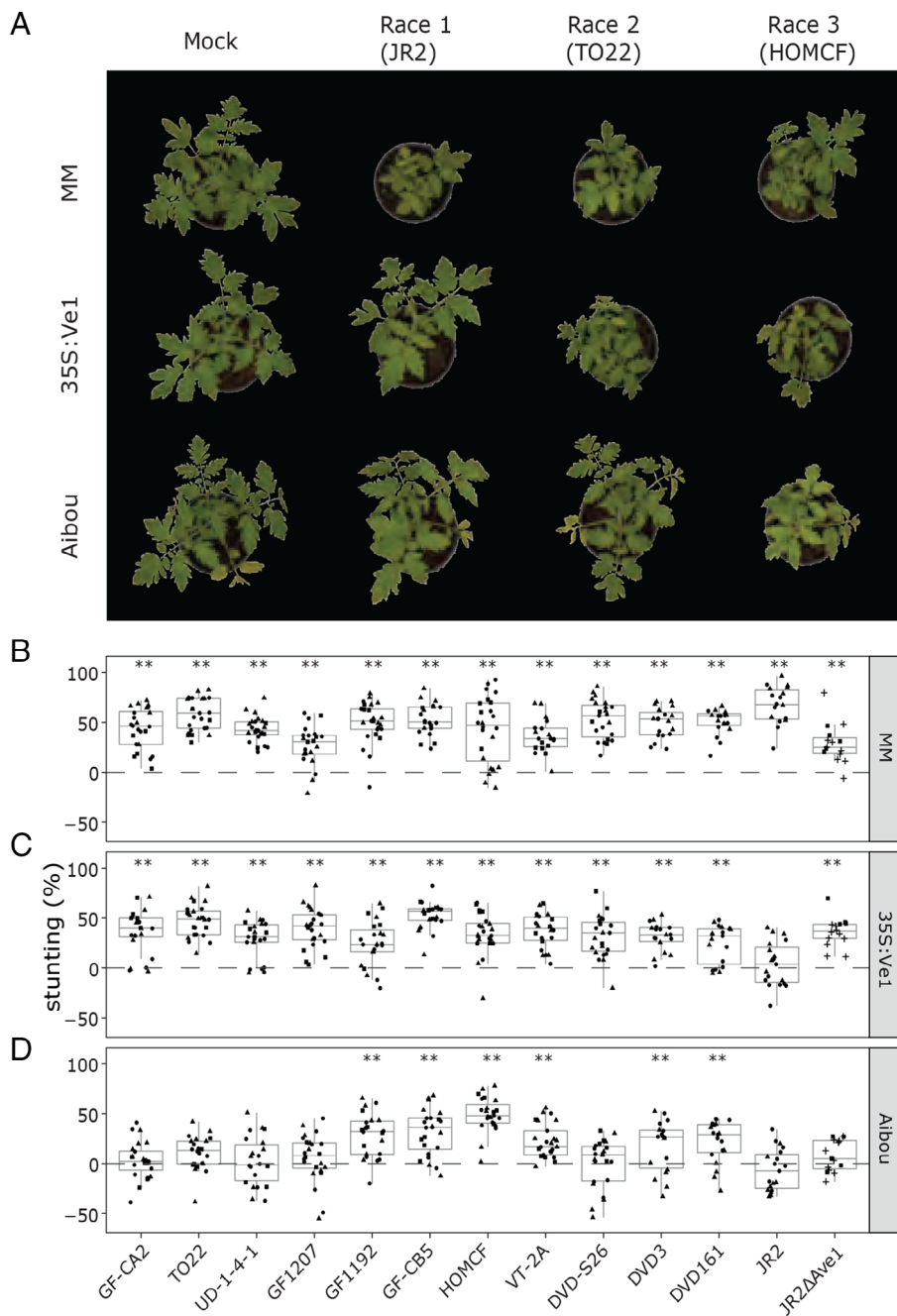


**Fig. 1.** Pathogenicity phenotyping of a collection of *Verticillium dahliae* strains on tomato.

A. Typical appearance of *V. dahliae* infection by strain JR2, TO22 and HOMCF as representatives for race 1, 2 and 3, respectively, on Moneymaker (MM) plants that lack known *V. dahliae* resistance genes, Ve1-transgenic Moneymaker plants that are resistant against race 1 and not against race 2 or 3 strains, and Aibou plants that carry Ve1 and V2 and are therefore resistant against race 1 as well as race 2 strains, but not against race 3 strains at 21 days post inoculation (dpi).

B–D. Measurement of *V. dahliae*-induced stunting on wild-type Moneymaker plants (B), Ve1-transgenic Moneymaker plants (35S:Ve1) (C) and Aibou plants (D) at 21 dpi. The graphs show collective data from four different experiments indicated with different symbols (circles, squares, triangles and plus symbols), and asterisks indicate significant differences between *V. dahliae*- and mock-inoculated plants as determined with an ANOVA followed by a Fisher's LSD test ( $P < 0.01$ ).

mapped against the *V. dahliae* strain JR2 genome assembly, and common genes were extracted. Sequences that did not map to the *V. dahliae* strain JR2 genome assembly were *de novo* annotated and signal peptides for secretion at the N-termini of the encoded proteins were predicted to identify potential effector genes.

Our strategy identified 563 kb of race 2-specific regions, containing 110 genes of which six encode putative secreted proteins, for scenario I (Table 2). For approach II,

222 kb of sequence that lacks in race 3 strains was identified with 40 genes of which only two are predicted to encode secreted proteins; *XLOC\_00170* (*VDAG\_JR2\_Chrg03680a*) and *evm.model.contig1569.344* (*VDAG\_JR2\_Chrg03650a*, further referred to as *Evm\_344*). Intriguingly, both these genes were previously recognized as being among the most highly expressed effector genes during colonization of *Nicotiana benthamiana* plants (de Jonge et al. 2013; Faino et al., 2015).

**Table 1.** *Verticillium dahliae* strains used in this study for comparative genomics and genome assembly statistics.

Strain	Previous race annotation	Ref. isolate <sup>a</sup>	Novel race annotation	Platform <sup>b</sup>	Data (Gb) <sup>c</sup>	Assembly size (Mb)	No. of contigs <sup>d</sup>	Contig N50 (Kb) <sup>4</sup>	Ref. sequencing <sup>a</sup>
JR2	1	A	1	PacBio	8.9	36.1	8	4168	D
DVDS26	2	B	2	Illumina	1	35.3	5361	47.1	B
DVD161	2	B	2, 3	Illumina	1	34.1	4078	42.4	B
DVD3	2	B	2, 3	Illumina	1	34.1	9318	43.9	B
TO22	2	C	2	Nanopore	4	34.9	20	12.4	TS
UD1-4-1	2	C	2	Nanopore	1.9	34.6	18	18.1	TS
GF1207	2	C	2	Nanopore	1.6	34.8	69	8.5	TS
GF-CA2	2	C	2	Nanopore	2	35	38	9.1	TS
GF-CB5	3	C	2, 3	Nanopore	4	34.8	19	11.4	TS
VT-2A	3	C	2, 3	Nanopore	1.8	34.8	22	10.2	TS
GF1192	3	C	2, 3	Nanopore	2	34.6	23	14.5	TS
HOMCF	3	C	2, 3	Nanopore	2	36.1	33	10.1	TS

<sup>a</sup>References: A: Fradin *et al.*, 2009; B: de Jonge *et al.*, 2012; C: Usami *et al.*, 2017; D: Faino *et al.*, 2015; TS: this study.<sup>b</sup>Sequencing platform used.<sup>c</sup>Amount of sequencing data generated.<sup>d</sup>For strains DVDS26, DVD161 and DVD3 previously determined scaffold statistics are shown (de Jonge *et al.*, 2012).**Table 2.** Comparative genomics of race 2 and race 3 strains.

Scenario	I	II
Reference strain	TO22	JR2
Race 2	GF-CA2	GF-CA2
	TO22	TO22
	UD-1-4-1	UD-1-4-1
	DVDS26	DVDS26
	GF1207	GF1207
Race 3	GF-1192	GF-1192
	GF-CB5	GF-CB5
	HOMCF	HOMCF
	DVD161	DVD161
	DVD3	DVD3
	VT-2A	VT-2A
Retained (kb)	563	222
Shared with JR2 (kb)	222	222
#JR2 genes	40	40
#Augustus-predicted genes	70	--
#Secreted	6	2
Retained candidates	<ul style="list-style-type: none"> <li>• XLOC_00170</li> <li>• evm.model.contig1569.344</li> </ul> <ul style="list-style-type: none"> <li>• tig00000058:1 027 588–1 028 906</li> <li>• tig00000058:1 116 044–1 116 494</li> <li>• tig00000151:403362–404 089</li> <li>• tig00017428:835657–837 290</li> </ul>	<ul style="list-style-type: none"> <li>• XLOC_00170</li> <li>• evm.model. contig1569.344</li> </ul>

### Only two of the Av2 candidates are expressed in planta

We anticipate that the genuine Av2 gene may not necessarily be expressed in *N. benthamiana* (de Jonge *et al.* 2013) but should be expressed particularly in tomato. Real-time PCR analysis on a time course of tomato cultivar Moneymaker plants inoculated with the *V. dahliae* JR2 strain revealed that the two candidate genes are expressed during tomato colonization, with a peak in expression around 7 days post inoculation, whereas little to no expression could be recorded upon growth *in vitro* (Fig. 2A). Both genes are similarly expressed in *V. dahliae* strain TO22, albeit that the expression peaks

slightly later, at 11 dpi (Fig. 2B). However, whereas the expression level of both genes is similar in *V. dahliae* strain JR2, *Evm\_344* is higher expressed than *XLOC\_00170* in *V. dahliae* strain TO22. Importantly, none of the four additional avirulence effector gene candidates that were identified in comparative genomics scenario I is expressed *in planta* in *V. dahliae* strain TO22 (Fig. 2B). Thus, based on the transcriptional profiling, these four avirulence effector genes can be disqualified as Av2 candidates, and only two genes that display an expression profile that can be expected for a potential avirulence effector gene remain; *XLOC\_00170* and *Evm\_344*.

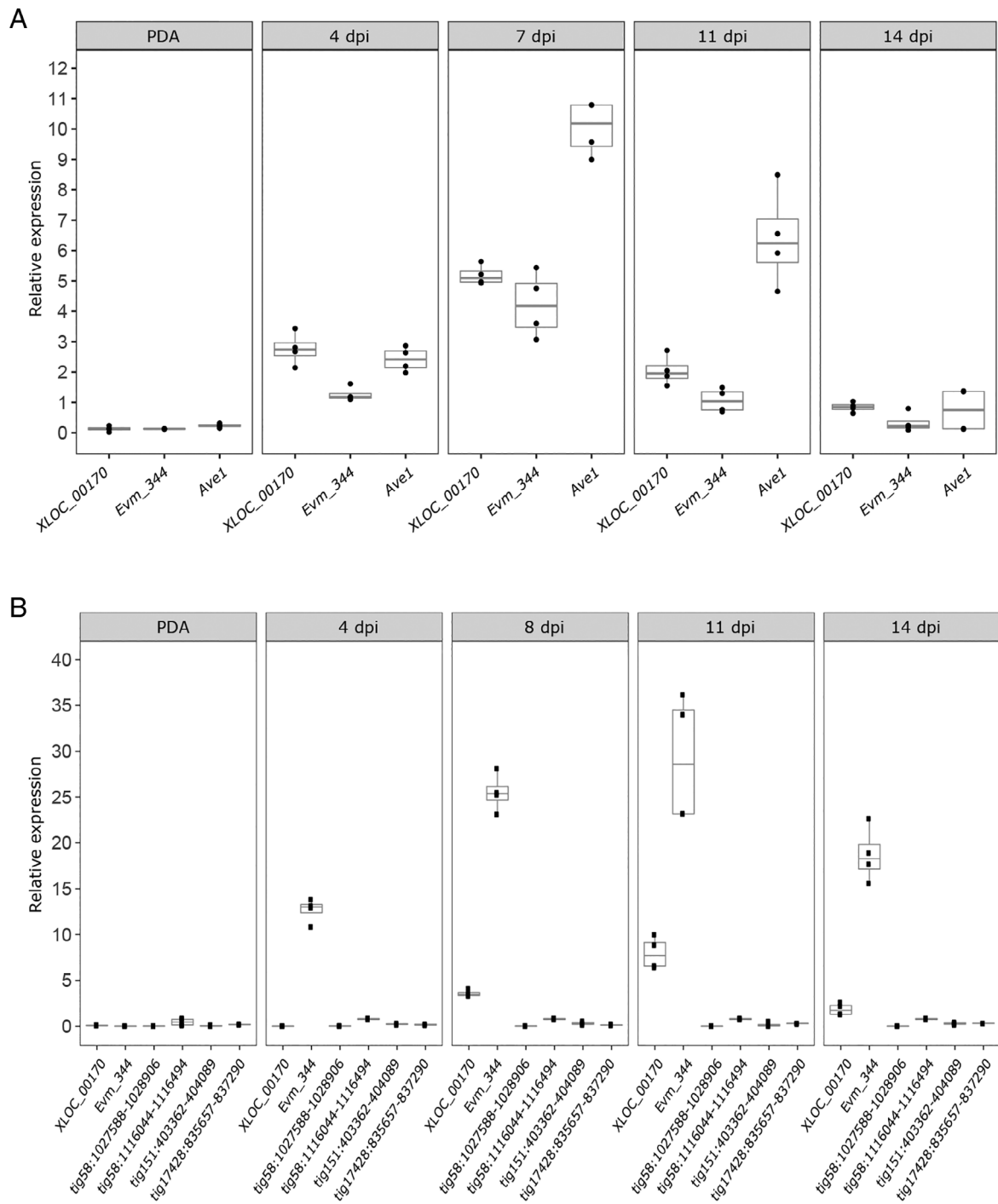


**Fig. 2.** Expression of *V. dahliae* candidate avirulence effector genes *in vitro* and during colonization of tomato plants. To assess *in planta* expression, 12-day-old tomato cv. Moneymaker seedlings were root-inoculated with *V. dahliae* strain JR2 (A) or strain TO22 (B), and plants were harvested from 4 to 14 days post inoculation (dpi), while conidiospores were harvested from 5-day-old cultures of *V. dahliae* on potato dextrose agar (PDA) to monitor *in vitro* expression. Real-time PCR was performed to determine the relative expression of XLOC\_00170, Evm\_344 and the race 1-specific effector gene VdAve1 as a positive control (de Jonge *et al.*, 2012) for strain JR2, using *V. dahliae* GAPDH as reference (A). Similarly, the relative expression of XLOC\_00170, Evm\_344 and six additional avirulence effector genes for strain TO22, using *V. dahliae* GAPDH as reference (B).

#### XLOC\_00170 encodes Av2

To identify which of the two candidates encodes Av2, a genetic complementation approach was pursued in which

the two candidate genes were introduced individually into the *V. dahliae* race 3 strains GF-CB5 and HOMCF. Subsequently, inoculations were performed on a differential

set of tomato genotypes, comprising Moneymaker plants, *Ve1*-transgenic Moneymaker plants (Fradin *et al.*, 2009), and Aibou plants (Usami *et al.*, 2017). As expected, the non-transformed race 3 strains GF-CB5 and HOMCF as well as the complementation lines containing *XLOC\_00170* or *Evm\_344* caused clear stunting of the universally susceptible Moneymaker as well as of the *Ve1*-transgenic Moneymaker plants (Fig. 3A and B). Interestingly, non-transformed race 3 strains GF-CB5 and HOMCF and the *Evm\_344* complementation lines caused clear stunting on Aibou plants, whereas the *XLOC\_00170* complementation lines did not induce disease symptoms and stunting on these plants (Fig. 3A and B). As such, these complementation transformants of the race 3 strains GF-CB5 and HOMCF behaved essentially as the race 2 strain TO22 (Fig. 3A and B). Thus, these findings suggest that *XLOC\_00170* encodes Av2. All visual observations of stunting were supported by quantifications of fungal biomass by real-time PCR (Fig. 3C). These measurements revealed that fungal biomass levels were only reduced on Aibou plants when inoculated with the race 2 strain TO22, and with the race 3 strains GF-CB5 and HOMCF that were complemented with *XLOC\_00170*. Thus, our data confirm that reduced symptomatology is accompanied by significantly reduced fungal colonization and indicate that *XLOC\_00170* encodes the race 2-specific avirulence effector Av2.

To further confirm that *XLOC\_00170* encodes Av2, targeted gene deletions were pursued in race 2 strain TO22 as well as in the JR2 $\Delta$ Ave1 strain and inoculations were performed on Moneymaker plants, *Ve1*-transgenic Moneymaker plants (Fradin *et al.*, 2009), and Aibou plants (Usami *et al.*, 2017). All *V. dahliae* genotypes caused clear stunting on wild-type and *Ve1*-transgenic Moneymaker plants, except for wild-type JR2 on *Ve1*-transgenic Moneymaker (Fig. 4A and B). Interestingly, whereas *V. dahliae* strains TO22 and JR2 $\Delta$ Ave1 were contained on Aibou plants, the *XLOC\_00170* deletion strains caused stunting of these plants in a similar fashion as the race 3 strains GF-CB5 and HOMCF (Fig. 4C). All visual observations were supported by quantification of biomass by real-time PCR (Fig. 4C). Collectively, our data unambiguously demonstrate that *XLOC\_00170* encodes the Av2 effector that is recognized on V2 tomato plants.

#### Av2 does not seem to contribute to virulence

It has been widely recognized that the intrinsic function of Avrs is to support host colonization by acting as virulence determinants (Jones and Dangl, 2006; Rovenich *et al.*, 2014; Cook *et al.*, 2015). Thus, we assessed the virulence of the complementation lines alongside their wild-type progenitor genotypes on wild-type and *Ve1*-transgenic

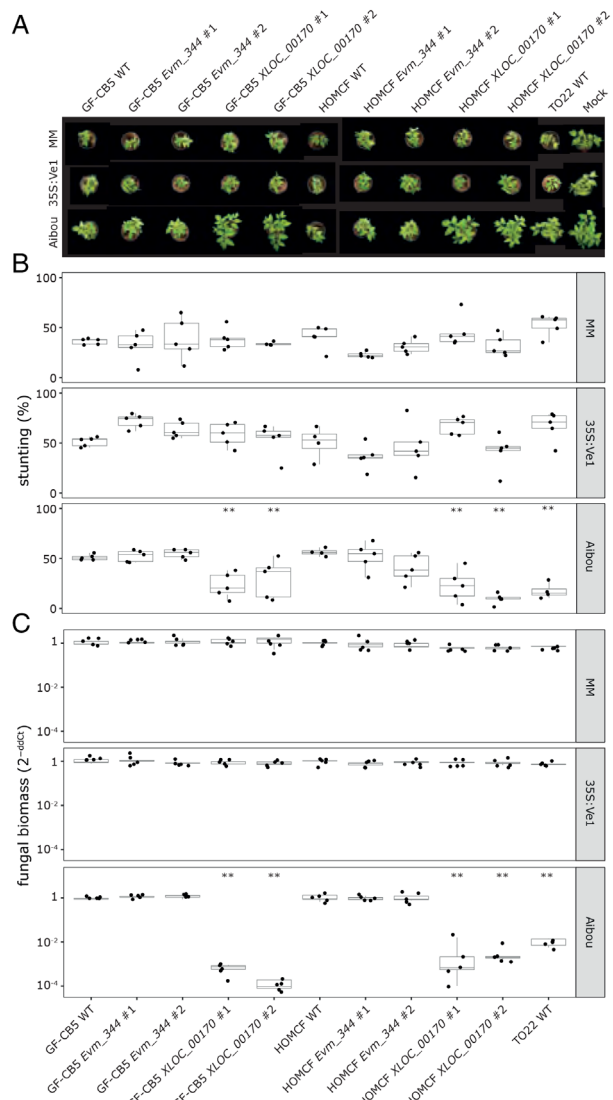


**Fig. 3.** Genetic complementation demonstrates that *XLOC\_00170* encodes the avirulence effector Av2 that is recognized in V2 plants. A. Top pictures of Moneymaker plants that lack known *V. dahliae* resistance genes (MM), *Ve1*-transgenic Moneymaker plants that are resistant against race 1 and not against race 2 strains of *V. dahliae* (MM 35S:Ve1), and Aibou plants that carry *Ve1* and V2 and are therefore resistant against race 1 as well as race 2 strains of the pathogen (Usami *et al.*, 2017) inoculated with the race 3 WT strains GF-CB5 and HOMCF, and two independent genetic complementation lines that express *XLOC\_00170* or *Evm\_344*, and the race 2 strain TO22. B. Quantification of stunting caused by the various *V. dahliae* genotypes on the various tomato genotypes as detailed for panel (A). Each combination is represented by the measurement of five plants. C. Quantification of fungal biomass with real-time PCR determined for the various *V. dahliae* genotypes on the various tomato genotypes as detailed for panel (A). Each combination is represented by the fungal biomass quantification in five plants. Asterisks indicate significant differences between *V. dahliae*- and mock-inoculated plants as determined with an ANOVA followed by a Fisher's LSD test ( $P < 0.01$ ).

Moneymaker plants (Fig. 3). However, no significant increase in symptomatology nor in fungal colonization could be recorded upon Av2 introduction. Similarly, no

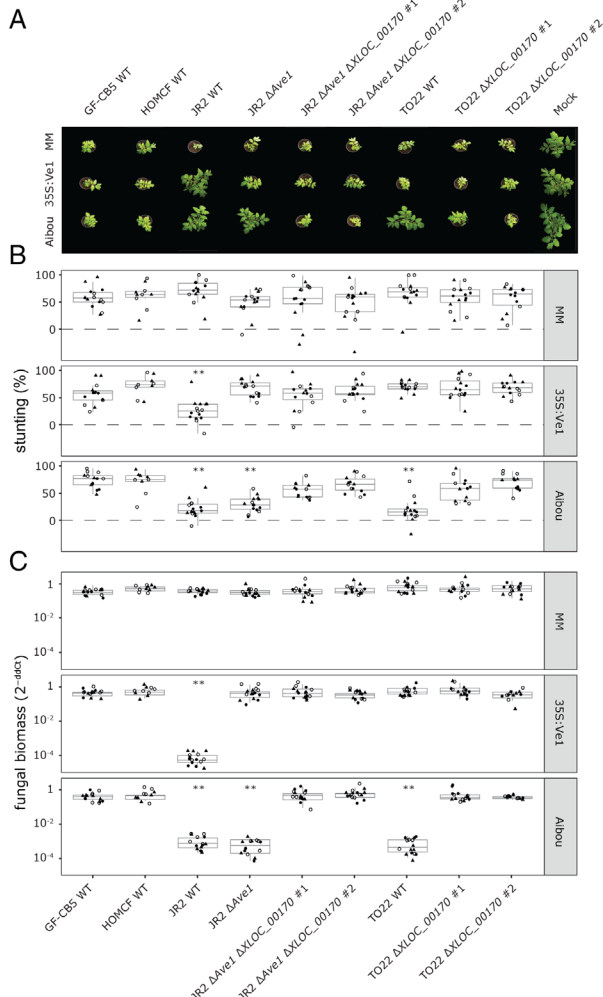


**Fig. 4.** Targeted deletion confirms that *XLOC\_00170* encodes the avirulence effector Av2 that is recognized in V2 plants. A. Top pictures of Moneymaker plants that lack known *V. dahliae* resistance genes (MM), *Ve1*-transgenic Moneymaker plants that are resistant against race 1 and not against race 2 strains of *V. dahliae* (35S:Ve1), and Aibou plants that carry *Ve1* and V2 and are therefore resistant against race 1 as well as race 2 strains of the pathogen (Usami *et al.*, 2017) inoculated with the race 3 strains GF-CB5 and HOMCF, the race 1 WT strain JR2, the deletion line JR2ΔAve1, two independent knock-out lines of *XLOC\_00170* in JR2ΔAve1, the race 2 WT strain TO22 and two independent knock-out lines of *XLOC\_00170* in TO22.

B. Quantification of stunting.

C. Quantification of fungal biomass with real-time PCR caused by the various *V. dahliae* genotypes on the various tomato genotypes as detailed for panel (A). Different symbols (empty circles, filled circles and triangles) refer to five plants from three different experiments. Asterisks indicate significant differences between *V. dahliae*- and mock-inoculated plants as determined with an ANOVA followed by a Fisher's LSD test ( $P < 0.01$ ).

significant decrease in symptomatology, nor a decrease in fungal colonization could be recorded upon Av2 deletion from *V. dahliae* strain TO22 on these tomato genotypes and upon Av2 deletion from JR2ΔAve1 on wild-type Moneymaker plants (Fig. 4), suggesting that Av2 is

not a major contributor to virulence on tomato under the conditions of our assays.

#### Av2 distribution and allelic variation

Av2 encodes a 91 amino acid protein that, after removal of a predicted signal peptide, leaves a mature protein of 73 amino acids that includes four cysteine residues and that lacks known protein domains. Intriguingly, an Av2 homologue is found in *V. nonalfalfa* (78% identity), *V. longisporum* (68% identity) and *V. alfalfa* (49%) that, like *V. dahliae*, belong to the Flavonexudans clade of *Verticillium* spp. (Fig. 5; Shi-Kunne *et al.*, 2018). Furthermore, BLAST searches revealed homologues in *Fusarium phyllophilum* (79% identity), *Fusarium mundagurra* (78%), *F. oxysporum* f. sp. *narcissi* (77%), *Fusarium oxysporum* NRRL32931 (75%), *F. oxysporum* f. sp. *pisi* (73%) and *Fusarium* sp. NRRL66182 (41%) (Fig. 5). No homologues are found in any of the other *Fusarium* spp nor in any other species.

To assess Av2 distribution in *V. dahliae*, presence-absence variations (PAV) were assessed in a collection of 52 previously sequenced *V. dahliae* strains (Fig. 6; de Jonge *et al.*, 2012; Faino *et al.*, 2015; Fan *et al.*, 2018; Gibriel *et al.*, 2019), revealing that Av2 occurred in 17 of the isolates including the four race 2 isolates that were sequenced in this study (Fig. 6). To assess the phylogenetic relationships between strains that carry Av2, a phylogenetic tree was generated, showing that the strains can be grouped into three major clades, two of which comprising strains that contain Av2. However, within these clades closely related strains occur that lost Av2, suggesting the occurrence of multiple independent losses (Fig. 6). Overall, no obvious phylogenetic structure is apparent with respect to effector presence within the *V. dahliae* population.

Next, we investigated the genomic organization surrounding Av2 based on the gapless genome assembly of *V. dahliae* strain JR2 (Faino *et al.*, 2015). Interestingly, Av2 resides in close proximity to *Evm\_344*, separated by only two additional genes, in a lineage-specific (LS) region on chromosome 4 (Fig. 7). Furthermore, as typically observed in LS regions that are enriched in repetitive elements (de Jonge *et al.*, 2013; Faino *et al.*, 2016), Av2 is surrounded by repetitive elements such as transposons that mostly belong to the class II long terminal repeat (LTR) retrotransposons (Fig. 7). Typically, LS regions are characterized by the high abundance of PAV. As expected, the flanking genomic regions (100 kb) are highly variable between *V. dahliae* strains (Fig. 7).

As many Avr effectors are under strong selection pressure and thus often display enhanced allelic variation (Stergiopoulos *et al.*, 2007), we assessed allelic variation among the 17 Av2 alleles identified in this study. We

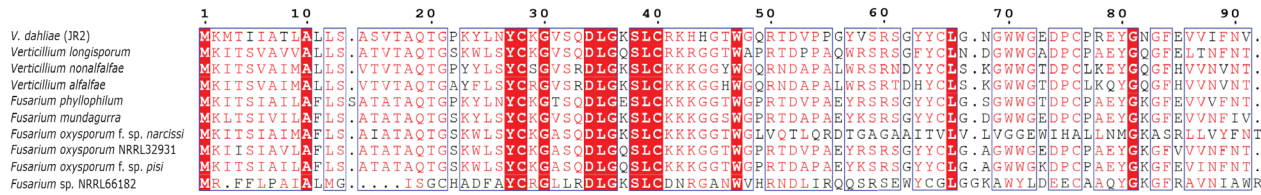


**Fig. 5.** Amino acid alignment of Av2 homologues found in few fungal species. Based on BLAST analyses, homologues of *V. dahliae* Av2 could only be identified in *V. longisporum*, *V. nonalfalfa*, *V. alalfa* and in *Fusarium phyllophilum*, *F. mundagurra*, three *F. oxysporum* lineages and in *Fusarium* sp. NRRL66182. Global alignments were performed using ClustalW and visualized with Esprits3. Conserved amino acids are shown in white font on red background.

identified only two allelic variants within the 17 Av2 alleles that differed by a single nucleotide polymorphism (SNP) in exon 3 leading to a polymorphic amino acid at position 73. Whereas 10 isolates carry a glutamic acid at this position (E<sub>73</sub>), seven other carry a valine (V<sub>73</sub>) (Fig. 8). Interestingly, strains carrying V<sub>73</sub> are clustered in the same branch, suggesting that a single event caused this polymorphism (Fig. 6). We noticed that all isolates carrying E<sub>73</sub> carry an extra transposable element of the DNA/Tc-1 Mariner class in the upstream region of the Av2 gene (Fig. 8). Intriguingly, as strains GF-CA2, TO22, UD-1-4-1 DVDS26 and GF1207, that encode the Av2 variant with V<sub>73</sub>, as well as JR2ΔAve1, that encodes the variant with E<sub>73</sub>, are contained on Aibou plants, we conclude that both allelic variants are recognized by V2. Moreover, the Av2 deletion strain of TO22 (with V<sub>73</sub>) as well as of JR2ΔAve1 (with E<sub>73</sub>) is not compromised in aggressiveness on wild-type Moneymaker plants when compared with the TO22 or JR2ΔAve1 progenitor strain, indicating that both alleles make no noticeable contribution to *V. dahliae* virulence.

## Discussion

Historically, the identification of avirulence genes has been challenging for fungi that reproduce asexually, as genetic mapping cannot be utilized. However, since the advent of affordable genome sequencing, cumbersome and laborious methods to identify avirulence genes, that include functional screenings of fungal cDNAs or protein fractions for the induction of immune responses in plants (Takken *et al.*, 2000; Luderer *et al.*, 2002), have been supplemented with comparative genomics and transcriptomics strategies (Gibriel *et al.*, 2016). Less than a decade ago, we identified the first avirulence gene of *V. dahliae*, known as VdAve1 for mediating avirulence on **Ve1** plants, through a comparative population genomics strategy combined with transcriptomics by utilizing race 1 strains that were contained by the **Ve1** resistance gene of tomato, and resistance-breaking race 2 strains (de Jonge *et al.*, 2013). In this study, we used a similar approach

based on comparative population genomics of race 1 and 2 strains with race 3 strains to successfully identify XLOC\_00170 as the Av2 effector that mediates avirulence on **V2** plants. Intriguingly, besides VdAve1, XLOC\_00170 has been identified previously as one of the most highly induced genes of *V. dahliae* during host colonization (de Jonge *et al.*, 2013).

Ve1 and the V2 locus are the only two major resistance sources that have been described in tomato against *V. dahliae* thus far (Fradin *et al.*, 2009; Usami *et al.*, 2017). Since its initial introduction from a wild Peruvian tomato accession into cultivars in the 1950s (Deseret News and Telegram, 1955), Ve1 has been widely exploited as it is incorporated in virtually every tomato cultivar today. Even though soon after the introduction of these cultivars resistance-breaking race 2 strains emerged, first in the United States (Robinson, 1957; Alexander, 1962), and soon thereafter also in Europe (Cirulli, 1969; Pegg and Dixon, 1969), Ve1 is still considered useful for *Verticillium* wilt control today. An important factor that contributes to the durability of resistance is the fitness penalty for the pathogen upon losing the corresponding avirulence factor (Brown, 2015). The VdAve1 effector contributes considerably to *V. dahliae* virulence on tomato, which explains why race 2 strains that lack VdAve1 are generally less aggressive (de Jonge *et al.*, 2012). Based on our current observations that differences in aggressiveness between race 2 and race 3 strains on Moneymaker plants are not obvious (Fig. 1), that genetic complementation of race 3 strains with Av2 did not lead to a striking increase in aggressiveness on Moneymaker plants (Fig. 3), and that targeted deletion of Av2 from race 2 strains did not lead to a striking decrease in aggressiveness on Moneymaker plants (Fig. 4), we conclude that the contribution of Av2 to *V. dahliae* virulence under the conditions tested in this study is modest at most.

Thus far, V2 resistance has been exploited scarcely when compared with Ve1, as it has only been introduced in a number of Japanese rootstock cultivars since 2006 (Usami *et al.*, 2017). Previously, V2 resistance-breaking race 3 strains have been found in several Japanese prefectures on two separate islands (Usami *et al.*, 2017).

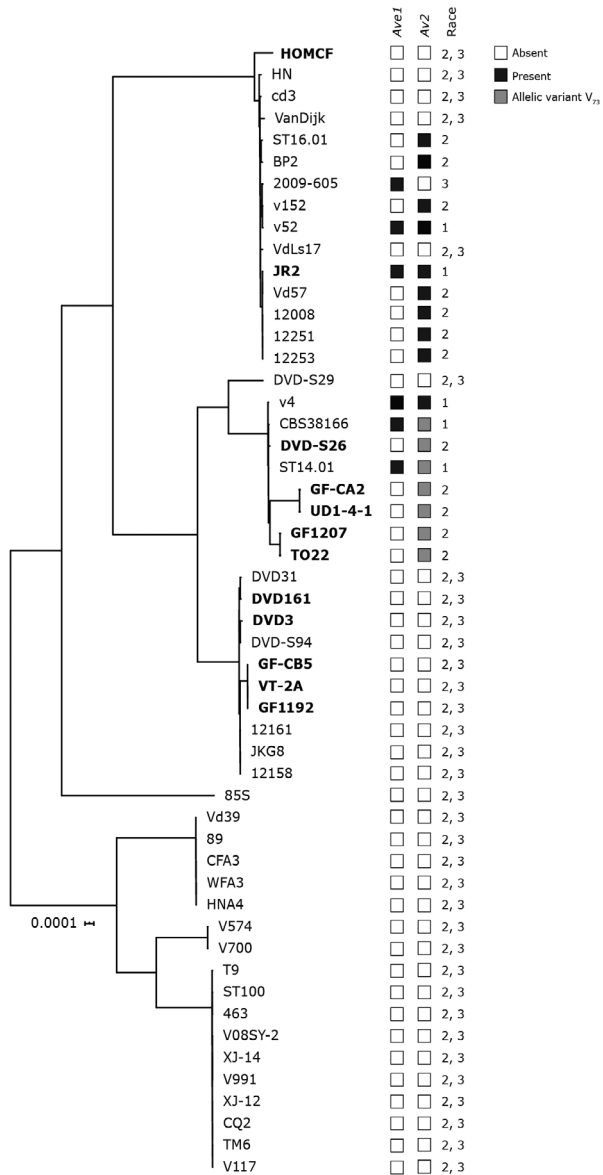


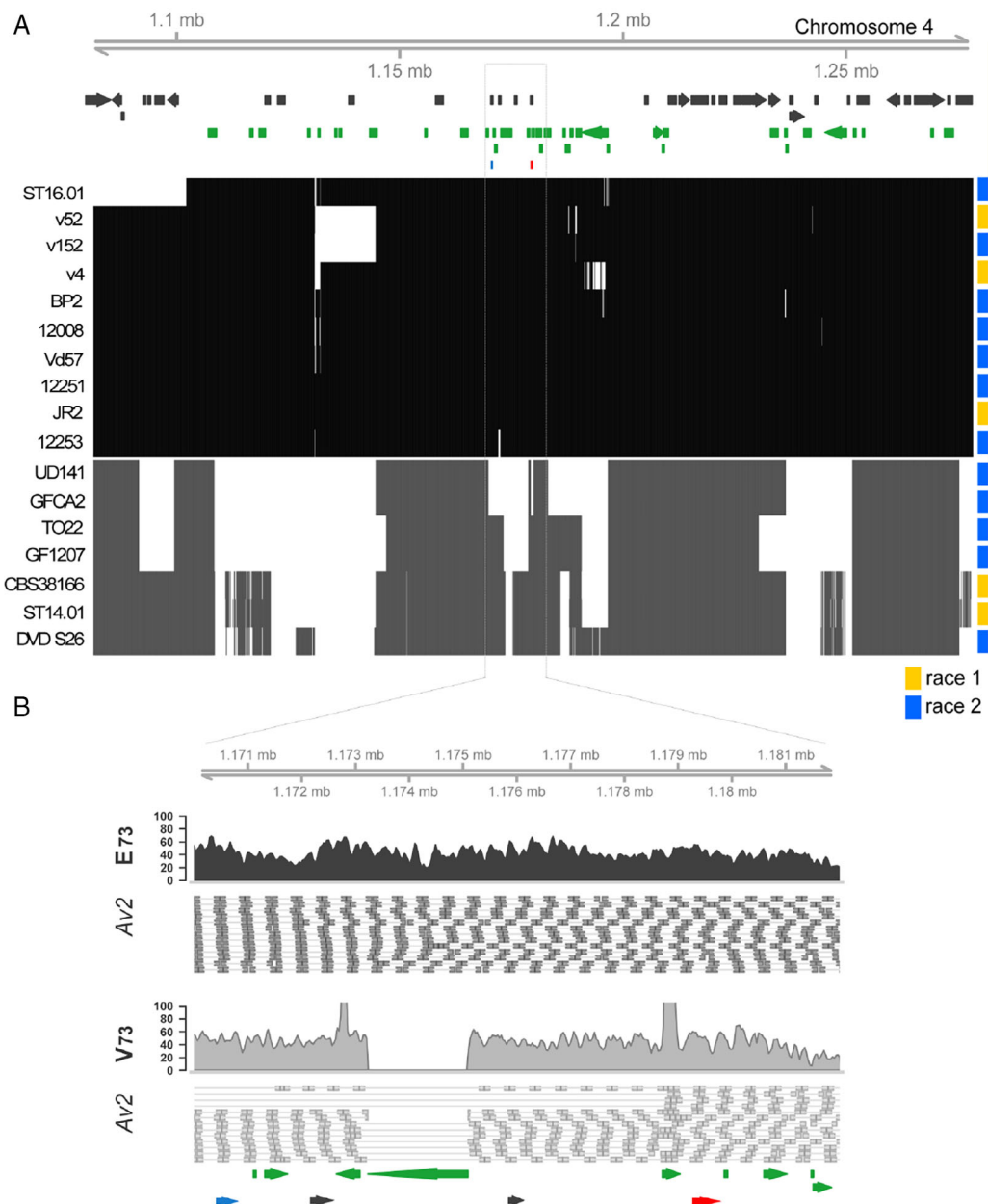
**Fig. 6.** Phylogenetic tree of sequenced *V. dahliae* strains with indication of presence-absence variation for the Ave1 and Av2 effectors. Strains that were phenotyped and included in the comparative genomics (Table 2) are shown in bold. Presence of the avirulence genes *VdAve1* and *Av2*, and the race designation based on the presence or absence of these genes are indicated. Phylogenetic relationships between sequenced *V. dahliae* strains were inferred using Realphy (Langmead and Salzberg, 2012), and branch length represents sequence divergence.

Intriguingly, our genome analyses demonstrate that race 3 strains that lack Av2 are ubiquitous and found worldwide, as our collection of sequenced strains comprises specimens that were originally isolated in Europe, China, Canada, and the United States. Arguably, most of these race 3 strains arose in the absence of V2 selection by tomato cultivation. It is conceivable that, similar to Ve1 homologues that are found in other plant species besides

tomato (Song *et al.*, 2017), functional homologues of V2 occur in other plant species as well, which may have selected against the presence of Av2 in many *V. dahliae* strains. However, as long as V2 is not cloned this hypothesis cannot be tested.

Like *VdAve1*, *Av2* also resides in an LS region of the *V. dahliae* genome, albeit in another region on another chromosome. Typically, these LS regions are gene-sparse and enriched in repetitive elements, such as transposons, causing these regions to be highly plastic which is thought to mediate accelerated evolution of effector catalogues (de Jonge *et al.*, 2013; Faino *et al.*, 2016; Cook, *et al.*, 2020). We previously demonstrated that *VdAve1* has been lost from the *V. dahliae* population multiple times, and to date only PAV has been identified as mechanism to escape *Ve1*-mediated immunity (de Jonge *et al.*, 2012, 2013; Faino *et al.*, 2016). Similarly, our phylogenetic analysis reveals that *Av2* has been lost multiple times independently, and although we identified two allelic variants, both variants are recognized by *V2*. Consequently, PAV remains the only mechanism to overcome *V2*-mediated immunity thus far. Despite the observation that PAV is the only observed mechanism for *V. dahliae* to overcome host immunity, pathogens typically exploit a wide variety of mechanisms, ranging from SNPs (Joosten *et al.*, 1994) to altered expression of the avirulence gene (Na and Gijzen, 2016). Nevertheless, avirulence gene deletion to overcome host immunity is common and has been reported for various fungi, including *C. fulvum* (Stergiopoulos *et al.*, 2007), *Fusarium oxysporum* (Niu *et al.*, 2016; Schmidt *et al.*, 2016), *Leptosphaeria maculans* (Gout *et al.*, 2007; Petit-Houdenot *et al.*, 2019), *Blumeria graminis* (Praz *et al.*, 2016) and *Magnaporthe oryzae* (Pallaghy *et al.*, 1994; Zhou *et al.*, 2007).

It was previously demonstrated that frequencies of SNPs are significantly reduced in the area surrounding the VdAve1 locus when compared with the surrounding genomic regions (Faino *et al.*, 2016), which was thought to point toward recent acquisition through horizontal transfer (de Jonge *et al.*, 2012). However, we recently noted that enhanced sequence conservation through reduced nucleotide substitution is a general feature of LS regions in *V. dahliae* (Depotter *et al.*, 2019). Although a mechanistic underpinning is still lacking, we hypothesized that differences in chromatin organization may perhaps explain this phenomenon. Interestingly, while DNA methylation is generally low and only present at TEs, only TEs in the core genome are methylated while LS TEs are largely devoid of methylation (Cook *et al.*, 2020). Furthermore, TEs within LS regions are more transcriptionally active and display increased DNA accessibility, representing a unique chromatin profile that could contribute to the plasticity of these regions (Faino *et al.*, 2016; Cook *et al.*, 2020). Possibly, the increased DNA accessibility

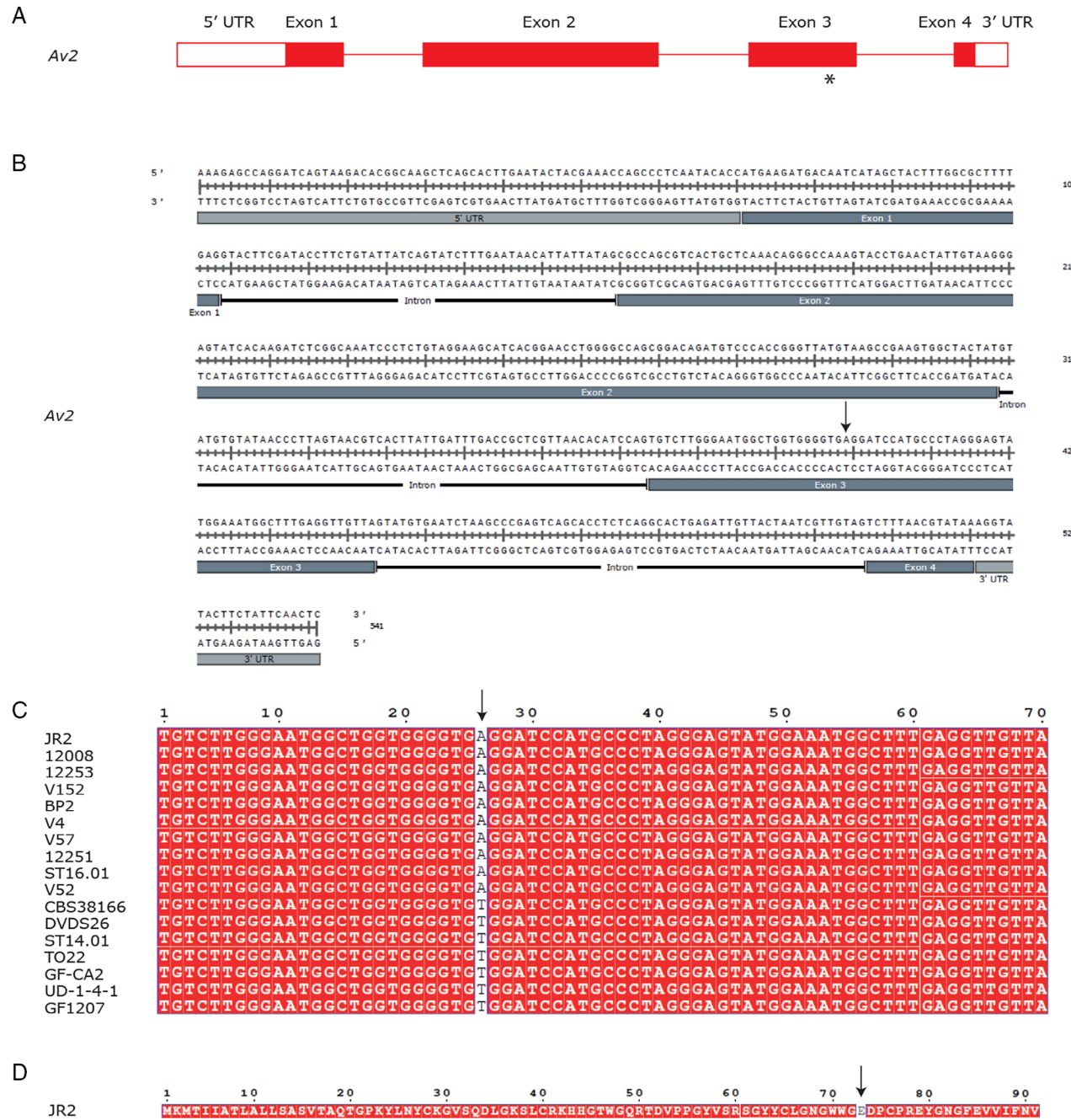


**Fig. 7.** Presence-absence variation in the region surrounding the two candidate Av2 genes (A) genomic region flanking the Av2 candidate genes in 17 isolates detailed in Fig. 3. The matrix shows the presence (black/grey) and absence (white) in 100 bp non-overlapping windows for Av2 variant *E*<sub>73</sub> (black) and Av2 variant *V*<sub>73</sub> grey. On top, annotated genes are displayed in black and repetitive elements in green, while Av2 is displayed in red and *Evm\_344* in blue. (B) Read coverage for *V. dahliae* strain JR2 that encodes Av2 variant *E*<sub>73</sub> and strain DVD-S26 that encodes Av2 variant *V*<sub>73</sub> depicting a transposable element deletion in isolates that produce the *V*<sub>73</sub> variant.

contributes to the high *in planta* expression of genes residing in these regions, and *VdAve1* as well as *Av2* belong to the most highly expressed genes during host colonization (de Jonge *et al.*, 2013).

Our identification of *Av2* concerns the cloning of only the second avirulence gene of *V. dahliae*. This identification may permit its use as a functional tool for genetic mapping of the *V2* gene. Typically, *V. dahliae* symptoms

on tomato display considerable variability, and disease phenotyping is laborious. Possibly, injections of heterologously produced *Av2* protein can be used to screen tomato plants in genetic mapping analyses, provided that such injections result in a visible phenotype such as a hypersensitive response. Similar effector-assisted resistance breeding has previously been used successfully to identify resistance sources in tomato against the leaf

**Fig. 8.** Allelic variation of Av2 in *Verticillium dahliae*.

A. Gene model for Av2. The asterisk indicates the approximate position of the single (A to T) nucleotide substitution in 7 of the 17 isolates that carry the gene, leading to a single amino acid substitution (E<sub>73</sub>V).

B. Genomic sequence of Av2. The arrow shows the position of the single nucleotide substitution found in particular strains.

C. Alignment of exon 3 of Av2 in the 17 strains containing the avirulence effector gene. The arrow shows the single nucleotide substitution that occurs in seven of the strains when compared with strain JR2.

D. Av2 amino acid sequence as encoded by *V. dahliae* strain JR2 with E<sub>73</sub> that is substituted by V in seven isolates indicated by an arrow.

mould pathogen *Cladosporium fulvum* (Lauge *et al.*, 1998; Takken *et al.*, 1999) and potato against the late blight pathogen *Phytophthora infestans* (Vleeshouwers and Oliver, 2014; Du *et al.*, 2015). The identification of

Av2 can furthermore be exploited for race diagnostics of *V. dahliae* to determine whether cultivation of resistant tomato genotypes is useful, but also to monitor *V. dahliae* population dynamics and race structures. Based on the

identification of avirulence genes, rapid in-field diagnostics can be developed to aid growers to cultivate disease-free crops.

## Materials and methods

### *V. dahliae* inoculation and phenotyping

Plants were grown in potting soil (Potgrond 4, Horticoop, Katwijk, the Netherlands) under controlled greenhouse conditions (Unifarm, Wageningen, the Netherlands) with day/night temperature of 24/18°C for 16-h/8-h periods, respectively, and relativity humidity between 50% and 85%. For *V. dahliae* inoculation, 10-day-old seedlings were root-dipped for 10 min as previously described (Fradin *et al.*, 2009). Disease symptoms were scored at 21 days post inoculation (dpi) by measuring the canopy area to calculate stunting as follows:

$$\text{stunting (\%)} = \left( 1 - \frac{\text{canopy area } V. dahliae - \text{inoculated plant}}{\text{average canopy area of mock - inoculated plants}} \right) * 100.$$

To test for significant stunting, an ANOVA was performed which tests for significant differences in canopy area between mock-inoculated and *V. dahliae* inoculated plants. Outliers were detected based on the studentized residuals from the ANOVA analysis. All datapoints with studentized residuals below -2.5 or above 2.5 were classified as outliers and removed. In total, approximately 1.8% of the datapoints were classified as outlier.

### High-molecular weight DNA isolation and nanopore sequencing

Conidiospores were harvested from potato dextrose agar (PDA) plates, transferred to Czapek dox medium and grown for 10 days. Subsequently, fungal material was collected on Miracloth, freeze-dried overnight and ground to powder with mortar and pestle of which 300 mg was incubated for 1 h at 65°C with 350 µl DNA extraction buffer (0.35 M Sorbitol, 0.1 M Tris-base, 5 mM EDTA pH 7.5), 350 µl nucleic lysis buffer (0.2 M Tris, 0.05 M EDTA, 2 M NaCl, 2% CTAB) and 162.5 µl Sarkosyl (10% w/v) with 1% β-mercaptoethanol. Next, 400 µl of phenol/chloroform/isoamyl alcohol (25:24:1) was added, shaken and incubated at room temperature (RT) for 5 min before centrifugation at 16 000 g for 15 min. After transfer of the aqueous phase to a new tube, 10 µl of RNAase (10 mg µL<sup>-1</sup>) was added and incubated at 37°C for 1 h. Subsequently, half a volume of chloroform was added, shaken and centrifuged at 16 000 g for 5 min at RT, after which the chloroform extraction was repeated. Next, the

aqueous phase was mixed with 10 volumes of 100% ice-cold ethanol, incubated for 30 min at RT, and the DNA was fished out using a glass hook, transferred to a new tube, and washed twice with 500 µl 70% ethanol. Finally, the DNA was air-dried, resuspended in nuclease-free water and incubated at 4°C for 2 days. The DNA quality, size and quantity were assessed by Nanodrop, gel electrophoresis and Qubit analyses.

Library preparation with the Rapid Sequencing Kit (SQK-RAD004) was performed according to the manufacturer's instructions (Oxford Nanopore Technologies, Oxford, UK) with 400 ng HMW DNA. An R9.4.1 flow cell (Oxford Nanopore Technologies) was loaded and run for 24 h. Base calling was performed using Guppy (version 3.1.5; Oxford Nanopore Technologies) with the high-accuracy base-calling algorithm. Adapter sequences were removed using Porechop (version 0.2.4 with default settings; Wick, 2018). Finally, the reads were self-corrected, trimmed and assembled using Canu (Version 1.8; Koren *et al.*, 2017). Sequencing data are available at the NCBI SRA database under accession number PRJNA639910.

### Comparative genomics and candidate identification

Self-corrected reads from *V. dahliae* race 3 strains were mapped against the reference genome using BWA-MEM (version 0.7.17; default settings; Li, 2013). Reads with low mapping quality (score < 10) were removed using Samtools view (version 1.9; setting: -q 10) (Li *et al.*, 2009), and reads mapping in regions with low coverage (<10x) were discarded using Bedtools coverage (version 2.25.0; setting: -d) (Quinlan and Hall, 2010). Self-corrected race 2 strain reads were mapped against the retained reference genome-specific regions that are absent from the race 3 strains. Retained sequences shared by the reference and every race 2 strain, while absent from every race 3 strain, were retained as Av2 candidate regions.

The previously determined annotation of *V. dahliae* strain JR2 (Faino *et al.*, 2015) was used to extract genes when JR2 or TO22 were used as alignment references. To this end, retained sequences shared by the TO22 reference assembly and race 2 strains, absent from race 3 strains, were mapped against the JR2 genome assembly, and genes in the shared sequences were extracted. The remaining sequences that did not map to the *V. dahliae* strain JR2 genome assembly were annotated using Augustus (version 2.1.5; default settings; Stanke *et al.*, 2006). SignalP software (version 4.0; Petersen *et al.*, 2011) was used to identify N-terminal signal peptides in predicted proteins.

### Real-time PCR

To determine expression profiles of Av2 candidate genes during *V. dahliae* infection of tomato, 2-week-old tomato

**Table 3.** Primers used in this study.

Primer name	Oligonucleotide sequence (5'→3')	Usage
XLOC00170-F	CAGCCCTCAATACACCATGAAGATG	qPCR
XLOC00170-R	TTCCGTGATGCTTCTACAGAGG	qPCR
evm1569.344-F	CACTGCTGGTTGCATGAT	qPCR
evm1569.344-R	TCCTTACTGTGCTGGATTCTG	qPCR
tig00000058-cdt1-F	GAGTGATGCTGTTGGTGTGG	qPCR
tig00000058-cdt1-R	AAGTCCGGATTGTCGAAC	qPCR
tig00000058-cdt2-F	CCACACCAACAGCATCACTC	qPCR
tig00000058-cdt2-R	CCTGCATCTGCATGTCAAGT	qPCR
tig00000151-F	TGTCGCGCTCTTGACTCT	qPCR
tig00000151-R	GTTGGCGTGGGTTCTACCTA	qPCR
tig00017428-F	CCATCCAGACCGAAACAAAGT	qPCR
tig00017428-R	CTGGAAGCCGCAGTTAGTC	qPCR
VdAve1-F	AGCTTCTACGCTTGG	qPCR
VdAve1-R	TTGGCTGGGATTGCT	qPCR
VdGAPDH-F	CGAGTCCACTGGTGTCTCA	qPCR
VdGAPDH-R	CCCTCAACGATGGTGAAC	qPCR
CO-XLOC00170-F	cgtctatataattaaATGAAAGATGACAATCATAGCTACTTGGC	Complementation
CO-XLOC00170-R	cgtctagccgcTTATACGTTAAAGACTACAACGATTAGTAACAATC	Complementation
CO-Evm344-F	cgtctatataattaaATGAAAATATCTTCCCATTACAGCC	Complementation
CO-Evm344-R	cgtctagccgcTTAGGAAGCTTCTTCGTCCTCG	Complementation
SIRUB-Fw	GAACAGTTCTCACTGTTGAC	qPCR
SIRUB-Rv	CGTGAGAACATAAGTCACC	qPCR
ITS1-F	AAAGTTTAATGGTCGCTAAGA	qPCR
STVe1-R	CTTGGTCATTTAGAGGAAGTAA	qPCR
JR2-XLOC170-LB-F	GGTCTTAAUAGAAGAATGTGGTGGGAGGA	Deletion
JR2-XLOC170-LB-R	GGCATTAAUTAGGGAAGGATGGCTGTTG	Deletion
JR2-XLOC170-RB-F	GGACTTAAUCGAAAGATAGACGTGTTGG	Deletion
JR2-XLOC170-RB-R	GGGTTAAUACGACGAGAGCCCTTATCAA	Deletion
TO22-XLOC170-F	GGTCTTAAUCAGCGTAATTTCGAGTGA	Deletion
TO22-XLOC170-RB-R	GGTCTTAAUGCTGATTTCCTTCGCGCATT	Deletion
TO22-XLOC170-LB-F	GGTCTTAAUTCGAAGGCAGATGTAACAA	Deletion
TO22-XLOC170-LB-R	GGTCTTAAUTGAGGGCTGGTTCGTAGT	Deletion

(cv. Moneymaker) seedlings were inoculated with *V. dahliae* strain JR2 or TO22, and stems were harvested up to 14 dpi. Furthermore, conidiospores were harvested from 5-day-old PDA plates. Total RNA extraction and cDNA synthesis were performed as previously described (Santhanam *et al.*, 2013). Real time-PCR was performed with primers listed in Table 3, using the *V. dahliae* glyceraldehyde-3-phosphate dehydrogenase gene (GAPDH) as endogenous control. The PCR cycling conditions were as follows: an initial 95°C denaturation step for 10 min followed by denaturation for 15 s at 95°C, annealing for 30 s at 60°C, and extension at 72°C for 40 cycles.

#### Genome mining

In total, 44 previously sequenced *V. dahliae* strains and eight strains sequenced in this study were mined for Av2 gene candidates using BLASTn. Gene sequences were extracted using Bedtools (setting: getfasta) (Quinlan and Hall, 2010) and aligned to determine allelic variation using Esprift (version 3.0; default settings) (Robert and Gouet, 2014). Similarly, amino acid sequences were aligned using Esprift (Robert and Gouet, 2014).

To determine the genomic localization of *XLOC\_00170* and *Evm\_344*, the *V. dahliae* strain JR2 assembly and

annotation were used (Faino *et al.*, 2015) together with coverage plots from reads of race 3 and race 2 strains as described in comparative genomics approach IV (Table 2) using R scripts, with the package karyoploteR for R (version 3.6) using kpPlotBAMCoverage function. The schematic representation of the genomic region on chromosome 4 with *XLOC\_00170* and *Evm\_344* was generated using Integrative Genomics Viewer (IGV) software v2.6.3 (Robinson *et al.*, 2011) and R package (version 3.6) Gviz (Hahne and Ivanek, 2016).

#### Phylogenetic tree construction

The phylogenetic tree of 52 *V. dahliae* strains was generated with Realphy (version 1.12) (Bertels *et al.*, 2014) using Bowtie2 (version 2.2.6) (Langmead and Salzberg, 2012) to map genomic reads against the *V. dahliae* strain JR2 assembly. A maximum likelihood phylogenetic tree was inferred using RAxML (version 8.2.8) (Stamatakis, 2014).

#### Presence–absence variation analysis

Presence–absence variation (PAV) was identified by using whole-genome alignments for 17 *V. dahliae* strains.

Paired-end short reads were mapped to *V. dahliae* strain JR2 (Faino *et al.*, 2015) using BWA-mem with default settings (Li and Durbin, 2009). Long-reads were mapped using minimap2 with default settings (Li, 2018). Using the Picard toolkit (<http://broadinstitute.github.io/picard/>), library artefacts were marked and removed with *-MarkDuplicates* followed by *-SortSam* to sort the reads. Raw read coverage was averaged per 100 bp non-overlapping windows using the BEDtools *-multicov* function (Quinlan and Hall, 2010). Next, we transformed the raw read coverage values to a binary matrix by applying a cut-off of 10 reads for short-read data;  $> = 10$  reads indicate presence (1) and  $< 10$  reads indicate absence (0) of the respective genomic region. For long-read data a cut-off of 1 read was used;  $> = 1$  read indicates presence (1) and  $< 1$  read indicates absence (0). The total number of PAV counts for each of the 100 bp genomic windows within 100 kb upstream and downstream of the candidate effectors was summarized.

#### Genetic complementation, deletion and functional analysis

For genomic complementation of race 3 strains GF-CB5 and HOMCF, a genomic construct was generated comprising the coding sequence of *XLOC\_00170* or *Evm\_344* in vector pFBT005 behind the *VdAve1* promoter, using primers CO-XLOC00170-F and CO-XLOC00170-R for *XLOC\_00170* or CO-Evm344-F and CO-Evm344-R for *Evm\_344* (Table 3).

For genomic deletion of *XLOC\_00170* from JR2 $\Delta$ Ave1 and race 2 strain TO22, a genomic construct was generated comprising the flanking regions of *XLOC\_00170* in vector pRF-NU2 (for JR2 $\Delta$ Ave1) or pRF-HU2 (for strain TO22), using primers JR2-XLOC170-LB-F, JR2-XLOC170-LB-R, JR2-XLOC170-RB-F and JR2-XLOC170-RB-R for strain JR2, and primers TO22-XLOC170-LB-F, TO22-XLOC170-LB-R, TO22-XLOC170-RB-F and TO22-XLOC170-RB-R for strain TO22 (Table 3).

*Agrobacterium tumefaciens*-mediated transformation (ATMT) was performed as described previously (Ökmen *et al.*, 2013) with a few modifications. *A. tumefaciens* was grown in 5 ml minimal medium (MM) supplemented with 50  $\mu\text{g m}^{-1}$  kanamycin at 28°C for 2 days. After subsequent centrifugation at 3000 g (5 min), cells were resuspended in 5 ml induction medium (IM) supplemented with 50  $\mu\text{g m}^{-1}$  kanamycin, adjusted to OD<sub>600</sub> 0.15 and grown at 28°C for minimum 6 h until OD<sub>600</sub> 0.5. Simultaneously, conidiospores of *V. dahliae* race 3 strains GF-CB5 and HOMCF were harvested after 1 week of cultivation on PDA plates with water, rinsed, and adjusted to a final concentration of 10<sup>6</sup> conidiospores mL<sup>-1</sup>. The *A. tumefaciens* suspension was mixed with *V. dahliae* conidiospores in a 1:1 volume ratio and 200  $\mu\text{l}$  of the mixture was spread onto

PVDF membranes in the centre of IM agar plates. After 2 days at 22°C, membranes were transferred to fresh PDA plates supplemented with 20  $\mu\text{g m}^{-1}$  nourseothricin and 200  $\mu\text{M}$  cefotaxime and incubated at 22°C for two weeks until *V. dahliae* colonies emerged. Transformants that appeared were transferred to fresh PDA supplemented with 20  $\mu\text{g m}^{-1}$  nourseothricin and 200  $\mu\text{M}$  cefotaxime. Successful transformation was verified by PCR and DNA sequencing.

*V. dahliae* inoculations were performed as described previously (Fradin *et al.*, 2009). Disease symptoms were scored 14 days after inoculation by measuring the canopy area to calculate stunting when compared with mock-inoculated plants. Outgrowth of *V. dahliae* from stem slices was assessed as described previously (de Jonge *et al.*, 2012). For biomass quantification, stems were freeze-dried and ground to powder, of which  $\sim$ 100 mg was used for DNA isolation. Real-time PCR was conducted with primers SIRUB-Fw and SIRUB-Rv for tomato *RuBisCo* and primers ITS1-F and STVe1-R for *V. dahliae* ITS (Table 3). Real-time PCR conditions were as follows: an initial 95°C denaturation step for 10 min followed by denaturation for 15 s at 95°C and annealing for 30 s at 60°C, and extension at 72°C for 40 cycles.

#### Acknowledgements

E.A.C.C. and D.T. acknowledge receipt of PhD fellowships from CONACyT. Work in the laboratories of B.P.H.J.T. and M.F.S. is supported by the Research Council for Earth and Life Science (ALW) of the Netherlands Organization for Scientific Research (NWO). B.P.H.J.T. acknowledges support by the Deutsche Forschungsgemeinschaft (DFG, German Research Foundation) under Germany's Excellence Strategy – EXC 2048/1 – Project ID: 390686111. Part of the work was funded by Foundation Topconsortium voor Kennis en Innovatie (TKI) Starting Materials, project number 1409-026.

#### Author contributions

J.P.V., T.U., M.F.S. and B.P.H.J.T. conceived the study; E.A.C.C., J.P.V., D.T., M.F.S. and B.P.H.J.T. designed experiments; E.A.C.C., J.P.V., D.T. performed experiments; E.A.C.C., J.P.V., D.T., H.J.S., Y.B., M.F.S. and B.P.H.J.T. analysed data, E.A.C.C., J.P.V. and B.P.H.J.T. wrote the manuscript; MFS and BPHJT supervised the project, all authors discussed the results and contributed to the final manuscript.

#### References

Alexander, L.J. (1962) Susceptibility of certain *Verticillium*-resistant tomato varieties to an Ohio isolate of the pathogen. *Phytopathology* **52**: 998–1000.  
 Anh, V.L., Inoue, Y., Asuke, S., Vy, T.T.P., Anh, N.T., Wang, S., *et al.* (2018) *Rmg8* and *Rmg7*, wheat genes for resistance to the wheat blast fungus, recognize the same

avirulence gene *AVR-Rmg8*. *Mol Plant Pathol* **19**: 1252–1256.

Baergen, K.D., Hewitt, J.D., and St. Clair, D.A. (1993) Resistance of tomato genotypes to four isolates of *Verticillium dahliae* race 2. *HortScience* **28**: 833–836.

Bertels, F., Silander, O.K., Pachkov, M., Rainey, P.B., and Van Nimwegen, E. (2014) Automated reconstruction of whole-genome phylogenies from short-sequence reads. *Mol Biol Evol* **31**: 1077–1088.

Bourras, S., Kunz, L., Xue, M., Praz, C.R., Müller, M.C., Kälin, C., et al. (2019) The AvrPm3-Pm3 effector-NLR interactions control both race-specific resistance and host-specificity of cereal mildews on wheat. *Nat Commun* **10**: 1–16.

Bourras, S., McNally, K.E., Ben-David, R., Parlange, F., Roffler, S., Praz, C.R., et al. (2015) Multiple avirulence loci and allele-specific effector recognition control the *Pm3* race-specific resistance of wheat to powdery mildew. *Plant Cell* **27**: 2991–3012.

Brown, J.K.M. (2015) Durable resistance of crops to disease: a Darwinian perspective. *Annu Rev Phytopathol* **53**: 513–539.

Chen, J., Upadhyaya, N.M., Ortiz, D., Sperschneider, J., Li, F., Bouton, C., et al. (2017) Loss of *AvrSr50* by somatic exchange in stem rust leads to virulence for *Sr50* resistance in wheat. *Science* **358**: 1607–1610.

Cirulli, M. (1969) Un isolato di *Verticillium dahliae* Kleb. virulento verso varietà resistenti di Pomodoro. *Phytopathol Mediterr* **8**: 132–136.

Cook, D.E., Kramer, M., Seidl, M.F., and Thomma, B.P. (2020) Chromatin features define adaptive genomic regions in a fungal plant pathogen. *BioRxiv* <https://dx.doi.org/10.1101/2020.01.27.921486>.

Cook, D.E., Mesarich, C.H., and Thomma, B.P.H.J. (2015) Understanding plant immunity as a surveillance system to detect invasion. *Annu Rev Phytopathol* **53**: 541–563.

Dangl, J.L., Horvath, D.M., and Staskawicz, B.J. (2013) Pivoting the plant immune system. *Science* **341**: 745–751.

Dangl, J.L., and Jones, J.D.G. (2001) Plant pathogens and integrated defence responses to infection. *Nature* **411**: 826–833.

Darvill, A.G., and Albersheim, P. (1984) Phytoalexins and their elicitors—a defense against microbial infection in plants. *Annu Rev Plant Physiol* **35**: 243–275.

de Jonge, R., Bolton, M.D., Kombrink, A., Van Den Berg, G.C.M., Yadeta, K.A., and Thomma, B.P.H.J. (2013) Extensive chromosomal reshuffling drives evolution of virulence in an asexual pathogen. *Genome Res* **23**: 1271–1282.

de Jonge, R., van Esse, H.P., Maruthachalam, K., Bolton, M.D., Santhanam, P., Saber, M.K., et al. (2012) Tomato immune receptor Ve1 recognizes effector of multiple fungal pathogens uncovered by genome and RNA sequencing. *Proc Natl Acad Sci U S A* **109**: 5110–5115.

Depotter, J.R.L., Shi-Kunne, X., Missonnier, H., Liu, T., Faino, L., van den Berg, G.C.M., et al. (2019) Dynamic virulence-related regions of the plant pathogenic fungus *Verticillium dahliae* display enhanced sequence conservation. *Mol Ecol* **28**: 3482–3495.

Deseret News and Telegram. (1955). From Jungles Of Peru. *Deseret News and Telegram*.

Diwan, N., Fluhr, R., Eshed, Y., Zamir, D., and Tanksley, S.D. (1999) Mapping of Ve in tomato: a gene conferring resistance to the broad-spectrum pathogen *Verticillium dahliae* race 1. *Theor Appl Genet* **98**: 315–319.

Dobinson, K.F., Tenuta, G.K., and Lazarovits, G. (1996) Occurrence of race 2 of *Verticillium dahliae* in processing tomato fields in southwestern Ontario. *Can J Plant Pathol* **18**: 55–58.

Dodds, P.N., and Rathjen, J.P. (2010) Plant immunity: towards an integrated view of plant-pathogen interactions. *Nat Rev Genet* **11**: 539–548.

Du, J., Verzaux, E., Chaparro-Garcia, A., Bijsterbosch, G., Keizer, L.C.P., Zhou, J., et al. (2015) Elicitin recognition confers enhanced resistance to *Phytophthora infestans* in potato. *Nat Plants* **1**: 1–5.

Faino, L., Seidl, M.F., Datema, E., van den Berg, G.C.M., Janssen, A., Wittenberg, A.H.J., and Thomma, B.P.H.J. (2015) Single-molecule real-time sequencing combined with optical mapping yields completely finished fungal genome. *mBio* **6**: 1–11.

Faino, L., Seidl, M.F., Shi-Kunne, X., Pauper, M., Van den, G.C., Wittenberg, A.H., and Thomma, B.P.H.J. (2016) Transposons passively and actively contribute to evolution of the two-speed genome of a fungal pathogen. *Genome Res* **26**: 1091–1100.

Fan, R., Cockerton, H.M., Armitage, A.D., Bates, H., Cascant-Lopez, E., Antanaviciute, L., et al. (2018) Vegetative compatibility groups partition variation in the virulence of *Verticillium dahliae* on strawberry. *PLoS One* **13**: 1–21.

Flor, H.H. (1942) Inheritance of pathogenicity in *Melampsora lini*. *Phytopathology* **32**: 653–669.

Fradin, E.F., and Thomma, B.P.H.J. (2006) Physiology and molecular aspects of *Verticillium* wilt diseases caused by *V. dahliae* and *V. albo-atrum*. *Mol Plant Pathol* **7**: 71–86.

Fradin, E.F., Zhang, Z., Juarez Ayala, J.C., Castroverde, C.D.M., Nazar, R.N., Robb, J., et al. (2009) Genetic dissection of *Verticillium* wilt resistance mediated by tomato Ve1. *Plant Physiol* **150**: 320–332.

Gout, L., Kuhn, M.L., Vincenot, L., Bernard-Samain, S., Cattolico, L., Barbetti, M., et al. (2007) Genome structure impacts molecular evolution at the *AvrLm1* avirulence locus of the plant pathogen *Leptosphaeria maculans*. *Environ Microbiol* **9**: 2978–2992.

Gibriel, H.A.Y., Li, J., Zhu, L., Seidl, M.F., and Thomma, B.P.H.J. (2019) *Verticillium dahliae* strains that infect the same host plant display highly divergent effector catalogs. *BioRxiv* <https://dx.doi.org/10.1101/528729>.

Gibriel, H.A.Y., Thomma, B.P.H.J., and Seidl, M.F. (2016) The age of effectors: genome-based discovery and applications. *Phytopathology* **106**: 1206–1212.

Hahne, F., and Ivanek, R. (2016) Visualizing genomic data using Gviz and Bioconductor. *Methods Mol Biol* **1418**: 335–351.

Inami, K., Yoshioka-Akiyama, C., Morita, Y., Yamasaki, M., Teraoka, T., and Arie, T. (2012) A genetic mechanism for emergence of races in *Fusarium oxysporum* f. sp. *lycopersici*: inactivation of avirulence gene *AVR1* by transposon insertion. *PLoS One* **7**: 1–10.

Inoue, Y., Vy, T.T.P., Yoshida, K., Asano, H., Mitsuoka, C., Asuke, S., et al. (2017) Evolution of the wheat blast fungus through functional losses in a host specificity determinant. *Science* **357**: 80–83.

Jones, J.D.G., and Dangl, J.L. (2006) The plant immune system. *Nature* **444**: 323–329.

Joosten, M.H.A.J., Cozijnsen, T.J., and de Wit, P.J.G.M. (1994) Host resistance to a fungal tomato pathogen lost by a single base-pair change in an avirulence gene. *Trends Genet* **10**: 117.

Kema, G.H.J., Mirzadi Gohari, A., Aouini, L., Gibriel, H.A.Y., Ware, S.B., Van Den Bosch, F., et al. (2018) Stress and sexual reproduction affect the dynamics of the wheat pathogen effector *AvrStb6* and strobilurin resistance. *Nat Genet* **50**: 375–380.

Klosterman, S.J., Atallah, Z.K., Vallad, G.E., and Subbarao, K.V. (2009) Diversity, pathogenicity, and management of *Verticillium* species. *Annu Rev Phytopathol* **47**: 39–62.

Koren, S., Walenz, B.P., Berlin, K., Miller, J.R., Bergman, N. H., and Phillippy, A.M. (2017) Canu: scalable and accurate long-read assembly via adaptive k-mer weighting and repeat separation. *Genome Res* **27**: 722–736.

Langmead, B., and Salzberg, S.L. (2012) Fast gapped-read alignment with bowtie 2. *Nat Methods* **9**: 357–359.

Lauge, R., Joosten, M.H.A.J., Haanstra, J.P.W., Goodwin, P. H., Lindhout, P., and de Wit, P.J.G.M. (1998) Successful search for a resistance gene in tomato targeted against a virulence factor of a fungal pathogen. *Proc Natl Acad Sci U S A* **95**: 9014–9018.

Li, H. (2013) Aligning sequence reads, clone sequences and assembly contigs with BWA-MEM. *ArXiv* **00**: 1–3.

Li, H. (2018) Minimap2: pairwise alignment for nucleotide sequences. *Bioinformatics* **34**: 3094–3100.

Li, H., and Durbin, R. (2009) Fast and accurate short read alignment with burrows-wheeler transform. *Bioinformatics* **25**: 1754–1760.

Li, H., Handsaker, B., Wysoker, A., Fennell, T., Ruan, J., Homer, N., et al. (2009) The sequence alignment/map format and SAMtools. *Bioinformatics* **25**: 2078–2079.

Lu, X., Kracher, B., Saur, I.M.L., Bauer, S., Ellwood, S.R., Wise, R., et al. (2016) Allelic barley MLA immune receptors recognize sequence-unrelated avirulence effectors of the powdery mildew pathogen. *Proc Natl Acad Sci U S A* **113**: E6486–E6495.

Luderer, R., Takken, F.L.W., de Wit, P.J.G.M., and Joosten, M.H.A.J. (2002) *Cladosporium fulvum* overcomes Cf-2-mediated resistance by producing truncated AVR2 elicitor proteins. *Mol Microbiol* **45**: 875–884.

Meile, L., Croll, D., Brunner, P.C., Plissonneau, C., Hartmann, F.E., McDonald, B.A., and Sánchez-Vallet, A. (2018) A fungal avirulence factor encoded in a highly plastic genomic region triggers partial resistance to septoria tritici blotch. *New Phytol* **219**: 1048–1061.

Mesarich, C.H., Griffiths, S.A., van der Burgt, A., Ökmen, B., Beenen, H.G., Etalo, D.W., et al. (2014) Transcriptome sequencing uncovers the Avr5 avirulence gene of the tomato leaf mold pathogen *Cladosporium fulvum*. *Mol Plant Microbe Interact* **27**: 846–857.

Na, R., and Gijzen, M. (2016) Escaping host immunity: new tricks for plant pathogens. *PLoS Pathog* **12**: 1–6.

Niu, X., Zhao, X., Ling, K.S., Levi, A., Sun, Y., and Fan, M. (2016) The *FonSIX6* gene acts as an avirulence effector in the *Fusarium oxysporum* f. sp. *Niveum* - watermelon pathosystem. *Sci Rep* **6**: 1–7.

Ökmen, B., Etalo, D.W., Joosten, M.H.A.J., Bouwmeester, H.J., de Vos, R.C.H., Collemare, J., and de Wit, P.J.G.M. (2013) Detoxification of  $\alpha$ -tomatine by *Cladosporium fulvum* is required for full virulence on tomato. *New Phytol* **198**: 1203–1214.

Pallaghy, P.K., Norton, R.S., Nielsen, K.J., and Craik, D.J. (1994) A common structural motif incorporating a cystine knot and a triple-stranded  $\beta$ -sheet in toxic and inhibitory polypeptides. *Protein Sci* **3**: 1833–1839.

Parlange, F., Daverdin, G., Fudal, I., Kuhn, M.L., Balesdent, M.H., Blaise, F., et al. (2009) *Leptosphaeria maculans* avirulence gene *AvrLm4-7* confers a dual recognition specificity by the *Rlm4* and *Rlm7* resistance genes of oilseed rape, and circumvents *Rlm4*-mediated recognition through a single amino acid change. *Mol Microbiol* **71**: 851–863.

Pegg, G.F., and Dixon, G.R. (1969) The reactions of susceptible and resistant tomato cultivars to strains of *Verticillium albo-atrum*. *Ann Appl Biol* **63**: 389–400.

Petersen, T.N., Brunak, S., Von Heijne, G., and Nielsen, H. (2011) SignalP 4.0: discriminating signal peptides from transmembrane regions. *Nat Methods* **8**: 785–786.

Petit-Houdenot, Y., Degrave, A., Meyer, M., Blaise, F., Ollivier, B., Marais, C.L., et al. (2019) A two genes – for – one gene interaction between *Leptosphaeria maculans* and *Brassica napus*. *New Phytol* **223**: 397–411.

Plissonneau, C., Daverdin, G., Ollivier, B., Blaise, F., Degrave, A., Fudal, I., et al. (2016) A game of hide and seek between avirulence genes *AvrLm4-7* and *AvrLm3* in *Leptosphaeria maculans*. *New Phytol* **209**: 1613–1624.

Praz, C.R., Bourras, S., Zeng, F., Sánchez-Martín, J., Menardo, F., Xue, M., et al. (2016) *AvrPm2* encodes an RNase-like avirulence effector which is conserved in the two different specialized forms of wheat and rye powdery mildew fungus. *New Phytol* **213**: 1301–1314.

Quinlan, A.R., and Hall, I.M. (2010) BEDTools: a flexible suite of utilities for comparing genomic features. *Bioinformatics* **26**: 841–842.

Robert, X., and Gouet, P. (2014) Deciphering key features in protein structures with the new ENDscript server. *Nucleic Acids Res* **42**: 320–324.

Robinson, D.B. (1957) *Verticillium Wilt of Potato in Relation to Symptoms, Epidemiology and Variability of the Pathogen*, Madison, WI: University of Wisconsin Agricultural Experiment Station Results Bulletin, p. 49.

Robinson, J.T., Thorvaldsdóttir, H., Winckler, W., Guttman, M., Lander, E.S., Getz, G., and Mesirov, J.P. (2011) Integrative Genome Viewer. *Nat Biotechnol* **29**: 24–26.

Rovenich, H., Boshoven, J.C., and Thomma, B.P.H.J. (2014) Filamentous pathogen effector functions: of pathogens hosts and microbiomes. *Curr Opin Plant Biol* **20**: 96–103.

Salcedo, A., Rutter, W., Wang, S., Akhunova, A., Bolus, S., Chao, S., et al. (2017) Variation in the *AvrSr35* gene determines *Sr35* resistance against wheat stem rust race Ug99. *Science* **358**: 1604–1606.

Santhanam, P., Van Esse, H.P., Albert, I., Faino, L., Nürnberger, T., and Thomma, B.P.H.J. (2013) Evidence for functional diversification within a fungal Nep1-like protein family. *Mol Plant Microbe Interact* **26**: 278–286.

Saur, I.M.L., Bauer, S., Kracher, B., Lu, X., Franzeskakis, L., Müller, M.C., et al. (2019) Multiple pairs of allelic MLA

immune receptor-powdery mildew AVR<sub>a</sub> effectors argue for a direct recognition mechanism. *EeLife* **8**: 1–31.

Schaible, L., Cannon, O.S., and Waddoups, V. (1951) Inheritance of resistance to *Verticillium* wilt in a tomato cross. *Phytopathology* **41**: 986–990.

Schmidt, S.M., Lukasiewicz, J., Farrer, R., van Dam, P., Bertoldo, C., and Rep, M. (2016) Comparative genomics of *Fusarium oxysporum* f. sp. *melonis* reveals the secreted protein recognized by the *Fom-2* resistance gene in melon. *New Phytol* **209**: 307–318.

Shan, W., Cao, M., Leung, D., and Tyler, B.M. (2004) The *Avr1b* locus of *Phytophthora sojae* encodes an elicitor and a regulator required for avirulence on soybean plants carrying resistance gene *Rps1b*. *Mol Plant Microbe Interact* **17**: 394–403.

Shi-Kunne, X., Faino, L., van den Berg, G.C.M., Thomma, B.P. H.J., and Seidl, M.F. (2018) Evolution within the fungal genus *Verticillium* is characterized by chromosomal rearrangement and gene loss. *Environ Microbiol* **20**: 1362–1373.

Snelders, N., Rovenich, H., Petti, G., Rocafort, M., Vorholt, J., Mesters, J., et al. (2020) A plant pathogen utilizes effector proteins for microbiome manipulation. *BioRxiv* <https://dx.doi.org/10.1101/2020.01.30.926725>.

Song, Y., Zhang, Z., Seidl, M.F., Majer, A., Jakse, J., Javornik, B., and Thomma, B.P.H.J. (2017) Broad taxonomic characterization of *Verticillium* wilt resistance genes reveals an ancient origin of the tomato Ve1 immune receptor. *Mol Plant Pathol* **18**: 195–209.

Stamatakis, A. (2014) RAxML version 8: a tool for phylogenetic analysis and post-analysis of large phylogenies. *Bioinformatics* **30**: 1312–1313.

Stanke, M., Tzvetkova, A., and Morgenstern, B. (2006) AUGUSTUS at EGASP: using EST, protein and genomic alignments for improved gene prediction in the human genome. *Genome Biol* **7**: 1–8.

Staskawicz, B.J., Dahlbeck, D., and Keen, N.T. (1984) Cloned avirulence gene of *Pseudomonas syringae* pv. *glycinea* determines race-specific incompatibility on *Glycine max* (L.) Merr. *Proc Natl Acad Sci U S A* **81**: 6024–6028.

Stergiopoulos, I., De Kock, M.J.D., Lindhout, P., and de Wit, P.J.G.M. (2007) Allelic variation in the effector genes of the tomato pathogen *Cladosporium fulvum* reveals different modes of adaptive evolution. *Mol Plant Microbe Interact* **20**: 1271–1283.

Stukenbrock, E.H., and McDonald, B.A. (2008) The origins of plant pathogens in agro-ecosystems. *Annu Rev Phytopathol* **46**: 75–100.

Takken, F.L.W., Luderer, R., Gabriëls, S.H.E.J., Westerink, N., Lu, R., De Wit, P.J.G.M., and Joosten, M. H.A.J. (2000) A functional cloning strategy, based on a binary PVX-expression vector, to isolate HR-inducing cDNAs of plant pathogens. *Plant J* **24**: 275–283.

Takken, F.L.W., Thomas, C.M., Joosten, M.H.A.J., Golstein, C., Westerink, N., Hille, J., et al. (1999) A second gene at the tomato Cf-4 locus confers resistance to *Cladosporium fulvum* through recognition of a novel avirulence determinant. *Plant J* **20**: 279–288.

Thomma, B.P.H.J., Nürnberger, T., and Joosten, M.H.A.J. (2011) Of PAMPs and effectors: the blurred PTI-ETI dichotomy. *Plant Cell* **23**: 4–15.

Usami, T., Momma, N., Kikuchi, S., Watanabe, H., Hayashi, A., Mizukawa, M., et al. (2017) Race 2 of *Verticillium dahliae* infecting tomato in Japan can be split into two races with differential pathogenicity on resistant rootstocks. *Plant Pathol* **66**: 230–238.

van Kan, J.A., van den Ackerveken, G.F., and de Wit, P.J. (1991) Cloning and characterization of cDNA of avirulence gene *avr9* of the fungal pathogen *Cladosporium fulvum*, causal agent of tomato leaf mold. *Mol Plant Microbe Interact* **4**: 52–59.

Vleeshouwers, V.G.A.A., and Oliver, R.P. (2014) Effectors as tools in disease resistance breeding against biotrophic, hemibiotrophic and necrotrophic plant pathogens. *Mol Plant Microbe Interact* **27**: 196–206.

Wick, R. (2018). *Porechop*. URL <https://github.com/rrwick/Porechop>

Zhong, Z., Marcel, T.C., Hartmann, F.E., Ma, X., Plissonneau, C., Zala, M., et al. (2017) A small secreted protein in *Zymoseptoria tritici* is responsible for avirulence on wheat cultivars carrying the *Stb6* resistance gene. *New Phytol* **214**: 619–631.

Zhou, E., Jia, Y., Singh, P., Correll, J.C., and Lee, F.N. (2007) Instability of the *Magnaporthe oryzae* avirulence gene *AVR-Pita* alters virulence. *Fungal Genet Biol* **44**: 1024–1034.